

## DECAY PROPERTIES AND STABILITY OF HEAVIEST ELEMENTS

A. V. KARPOV\* and V. I. ZAGREBAEV

*Flerov Laboratory of Nuclear Reactions, JINR, Dubna 141980, Russia*  
\*karpov@jinr.ru

Y. MARTINEZ PALENZUELA, L. FELIPE RUIZ and WALTER GREINER

*Frankfurt Institute for Advanced Studies, J. W. Goethe University,  
Frankfurt am Main 60438, Germany*

Received 15 December 2011

Accepted 9 January 2012

Published 1 March 2012

Decay properties and stability of heaviest nuclei with  $Z \leq 132$  are studied within the macro-microscopical approach for nuclear ground state masses and phenomenological relations for the half-lives with respect to  $\alpha$ -decay,  $\beta$ -decay and spontaneous fission. We found that at existing experimental facilities the synthesis and detection of nuclei with  $Z > 120$  produced in fusion reactions may be difficult due to their short half-lives (shorter than  $1 \mu\text{s}$ ). The nearest (more neutron-rich) isotopes of superheavy elements with  $111 \leq Z \leq 115$  to those synthesized recently in Dubna in  $^{48}\text{Ca}$ -induced fusion reactions are found to be  $\beta^+$ -decaying. This fact may significantly complicate their experimental identification. However it gives a chance to synthesize in fusion reactions the most stable superheavy nuclei located at the center of the island of stability. Our calculations yield that the  $\beta$ -stable isotopes  $^{291}\text{Cn}$  and  $^{293}\text{Cn}$  with a half-life of about 100 years are the longest-living superheavy nuclei located at the island of stability.

*Keywords:* Superheavy nuclei; decay modes; half-lives; alpha-decay; beta-decay; spontaneous fission.

### 1. Introduction

Great success was achieved during the last twenty years in the experimental study of reactions leading to superheavy nuclei, their decay properties and structure. Up to now near-barrier fusion reactions have been used for the production of new superheavy (SH) elements in the “cold”<sup>1–3</sup> and “hot”<sup>4</sup> combinations of colliding nuclei. However in the cold fusion reactions based on the closed shell target nuclei lead and bismuth the fusion cross-sections decrease very rapidly with increasing charge and mass of the projectile. The “world record” of 0.03 pb for the production cross-section of the element 113 has been obtained within more than a half-year irradiation of  $^{209}\text{Bi}$  target with  $^{70}\text{Zn}$  beam.<sup>2,3</sup>

For more asymmetric (and “hotter”) fusion reactions of  $^{48}\text{Ca}$  with actinide targets the cross-sections were found to be much larger.<sup>4,5</sup> However, californium is the heaviest available target which has been used in these experiments for the production of element 118.<sup>6</sup> Thus, to get SH elements with  $Z > 118$  in fusion reactions, one should proceed to heavier than  $^{48}\text{Ca}$  projectiles ( $^{50}\text{Ti}$ ,  $^{54}\text{Cr}$ , etc.). The corresponding cross-sections for the production of the elements 119 and 120 are predicted to be smaller by two orders of magnitude<sup>7</sup> as compared with  $^{48}\text{Ca}$ -induced fusion reactions leading to the formation of the elements 114–116. Another limitation of the fusion reactions (both “cold” and “hot”) for producing superheavy elements consists in the fact that they lead to neutron-deficient isotopes having rather short life time. However, the most stable superheavies are predicted to be located along the  $\beta$ -stability line in the region of more neutron-rich nuclei, which is unreachable by fusion reactions with stable beams. In fact, the predicted magic numbers, especially for protons, are quite different within different theoretical approaches. The magic number  $Z = 114$  was predicted in earliest macro-microscopic calculations<sup>8–11</sup> and confirmed later in Refs. 12, 13. The fully microscopic approaches predict the proton shell closure at  $Z = 120$ ,<sup>14</sup>  $Z = 126$ ,<sup>15</sup> or  $Z = 114, 120, 126$  (see Ref. 16) depending on the chosen nucleon–nucleon interaction in meson field theory. The neutron magic number  $N = 184$  is almost firmly predicted by different theoretical models.

Nowadays the experimental study of heavy nuclei, in particular of superheavies, requires ideas, new theoretical predictions, and methods (reactions) that can be used for producing these nuclides. Note, that it was found that the multi-nucleon transfer reactions might be used for the synthesis of long-living heavy neutron-enriched nuclei located on the island of stability.<sup>7,17,18</sup> On the other hand, knowledge of the decay modes and half-lives of nuclei in a very wide range of neutron and proton numbers (nuclear map) is necessary for such predictions and for the planning of the corresponding experiments. For example, at the existing experimental facilities, the registration of superheavy recoil in the focal plane of detectors is possible only if its half-life is longer than  $1 \mu\text{s}$ . This experimental limitation makes some regions of the nuclear map currently inaccessible to experimental studies. Another field where the decay properties play a crucial role is the study of the  $r$ -process of nucleosynthesis in the superheavy mass region, and the related problem of a search of superheavy nuclei in nature.

The main decay modes of heavy and superheavy nuclei are:  $\alpha$ -decay,  $\beta$ -decay, and spontaneous fission (SF). All the theoretical estimations of the half-lives against their main decay modes are based on the ground state masses and potential energy properties. There is a quite long history of the decay modes study,  $\alpha$ -decays were studied in a great number of works. The  $\alpha$ -decay half-lives are usually calculated within the Geiger–Nuttall-type formula (see, e.g. Refs. 19–21), within semi-empirical relations (e.g. Ref. 22) or using the WKB method (e.g. Refs. 23 and 24). The key quantity in all these methods is the energy of  $\alpha$ -decay, uncertainty which

mainly influences the accuracy of the calculations. These methods are rather simple giving comparable and good agreement with the experiment. In this paper, we apply a variant of Viola–Seaborg relation for  $\alpha$ -decay half-life. Estimation of  $\beta$ -decay half-life is more complicated, especially for nuclei close to the line of  $\beta$ -stability, where the half-life is strongly sensitive to the structure of the mother and daughter nuclei as well as to the corresponding  $Q$ -value. Systematic study of the  $\beta$ -decay half-lives was performed, e.g. in Refs. 25 and 26 restricting to allowed  $\beta$ -transitions. Phenomenological relations for  $\beta$  half-lives, such as the well-known Sargent law<sup>27,28</sup> or more recent parametrizations,<sup>29,30</sup> could be also very useful. The most uncertain quantity is the half-life of SF. This is due to more complicated and less understood fission dynamics and also due to much smaller experimental data on fission decays in comparison with  $\alpha$ - and  $\beta$ -decays. The main two methods applied for calculation of the SF half-lives are the phenomenological one<sup>31–33</sup> and more complicated dynamical approaches<sup>10,11,34–38</sup> (see below).

As said above, further researches in the region of superheavy nuclei require the knowledge of the decay properties (half-lives and modes of decay) of individual nuclei and their trends. This assumes that the main modes, i.e.  $\alpha$ -decay,  $\beta$ -decay, and SF, have to be calculated simultaneously. This paper is aimed to the analysis of the decay properties of heavy and superheavy elements with respect to all the three main decay modes. In Sec. 2 the details of the performed calculations are given. The main output of the calculations, i.e. the nuclear map containing the decay properties and half-lives of heavy and superheavy nuclei with  $Z \leq 132$ , is discussed in Sec. 3.

## 2. The Model

### 2.1. Nuclear masses

All the theoretical approaches used for the calculation of the nuclear masses as a function of collective degrees of freedom can be divided into three groups: macro-microscopical approach (see below), the generalized Thomas–Fermi method (e.g. Ref. 39), and microscopic approaches based on the self-consistent Hartree–Fock model (both relativistic and nonrelativistic) (e.g. Refs. 40 and 41). The macro-microscopical approach to the calculation of nuclear masses is widely used giving as a rule similar or even better agreement with the experiments than various “more fundamental” microscopic approaches.

The macro-microscopical approach is based on the assumption that the mass (depending on nucleon composition  $Z, N$  and deformation) can be obtained as a sum of two terms

$$M(Z, A, \text{def.}) = M_{\text{macro}}(Z, A, \text{def.}) + \delta U(Z, N, \text{def.}), \quad (1)$$

where the first term  $M_{\text{macro}}$  describes the gross dependence of the mass. Often, it is calculated by a variant of the liquid-drop model. The second term  $\delta U$  takes into account the influence of the shell structure on the mass. The Strutinsky

renormalization method<sup>42,43</sup> is usually applied for the calculation of the shell correction  $\delta U$ . The main part of the Strutinsky method is a single-particle Hamiltonian determining the spectra. The main difference of various macro-microscopical models consists in the different choice of the mean-field potential entering the Hamiltonian. The three mean-field potentials usually used are: convoluted Yukawa potential (see Refs. 26 and 44 and reference therein), (Woods–Saxon potential<sup>45–50</sup>), and two-center shell-model potential.<sup>51,52</sup>

All the calculations obtained in this paper are based on the values of the ground state masses. Of course all predictions made below in the experimentally unknown region are model dependent. Here we use experimental masses for known nuclei and the set of the ground state masses, obtained by Möller with collaborators<sup>44</sup> for unknown ones. This model (the droplet model for the macroscopic part and the folded Yukawa mean-field potential for the shell correction calculation) is one of the most known and tested, that makes our prediction rather reliable.

## 2.2. *Alpha-decay*

The  $\alpha$ -decay is characterized by the energy release  $Q_\alpha$  and the corresponding half-life  $T_\alpha$ . The value of  $Q_\alpha$  is given by

$$Q_\alpha = M_{\text{gs}}(Z, A) - M_{\text{gs}}(Z - 2, A - 4) - M_\alpha, \quad (2)$$

where  $M_\alpha$  is the mass of the  $\alpha$ -particle.

The half-life for  $\alpha$ -decay can be estimated quite accurately using the well-known Viola–Seaborg formula<sup>53</sup>

$$\log_{10} T_\alpha (\text{sec}) = \frac{aZ + b}{\sqrt{Q_\alpha (\text{MeV})}} + cZ + d + h_{\log}, \quad (3)$$

where  $a$ ,  $b$ ,  $c$ ,  $d$ , and  $h_{\log}$  are adjustable parameters. We use the values of these parameters obtained in Ref. 19  $a = 1.66175$ ,  $b = -8.5166$ ,  $c = -0.20228$ ,  $d = -33.9069$ . The quantity  $h_{\log}$  takes into account hindrance of  $\alpha$ -decay for nuclei with odd neutron and/or proton numbers<sup>53</sup>

$$h_{\log} = \begin{cases} 0, & Z \text{ and } N \text{ are even} \\ 0.772, & Z \text{ is odd and } N \text{ is even} \\ 1.066, & Z \text{ is even and } N \text{ is odd} \\ 1.114, & Z \text{ and } N \text{ are odd.} \end{cases} \quad (4)$$

The phenomenological calculation of  $T_\alpha$  is the most justified (among other decay-modes) and the most accurate. The errors arising from uncertainty in  $Q_\alpha$  are much larger than the one due to the inaccuracy of the phenomenological Viola–Seaborg formula.

## 2.3. *Beta-decay*

If one moves aside the stability line, the  $\beta$ -processes start to play an important role. Therefore, to estimate correctly the life time of such a nucleus we have to

consider the competition of  $\alpha$ -decay and spontaneous fission with  $\beta^\pm$  decays and the electron capture (EC). The decay properties of nuclei close to the  $\beta$ -stability line are mostly known (except for the region of superheavy nuclei). This means that we may restrict ourselves to the case of nuclei far from the line of  $\beta$ -stability. It allows us to assume that the corresponding  $Q$ -value and the density of states are large enough to find in the daughter nucleus a level which is close to the ground state and which fulfils the conditions of allowed  $\beta$ -decays. Thus, the problem simplifies to the case of the ground-to-ground allowed  $\beta$  transitions. This assumption may be not accurate enough for some specific nuclei close to the  $\beta$ -stability line, but this cannot alter the general trend in the decay modes, which we are interested in.

In the description we follow formulas and notations according to Refs. 28, 54 and 55. The half-life with respect to all kinds of  $\beta$  processes  $T_\beta$  is given by

$$1/T_\beta = 1/T_{\beta^+} + 1/T_{\beta^-} + 1/T_{EC}. \quad (5)$$

The half-life with respect to a specific type of decay is defined by the following relation:

$$f_0^b T_b = \ln\{2\} \left( \frac{g^2 m_e^5 c^4}{2\pi^3 \hbar^7} |M_{if}|^2 \right)^{-1}, \quad (6)$$

where  $f_0^b$  is the Fermi function,  $b = \beta^\pm$  or  $EC$ ;  $m_e$  is the electron mass and  $M_{if}$  is the corresponding transition matrix element between the initial (i) and final (f) states. The r.h.s. of (6) may be approximated by a constant for each kind of  $\beta$ -decay (allowed or forbidden of the different kind). In particular for the allowed  $\beta$ -decays one may use<sup>56</sup>

$$\log_{10} [f_0^b T_b (\text{sec})] = 5.7 \pm 1.1. \quad (7)$$

Thus, the estimation of the  $\beta$ -decay half-lives is reduced to the calculation of the Fermi function  $f_0^b$ . We use in (7) the constant value 4.7 (see below).

### 2.3.1. $\beta^\pm$ decays

The energy release in the case of  $\beta^-$  ground state to ground state decay is given by the mass difference

$$Q_{\beta^-} = M(A, Z) - M(A, Z + 1), \quad (8)$$

while for the  $\beta^+$ -decay it is

$$Q_{\beta^+} = M(A, Z) - M(A, Z - 1) - 2m_e c^2. \quad (9)$$

The Fermi function  $f_0^{\beta^\pm}$  is given by

$$f_0^{\beta^\pm} = \int_1^{E_0} F(E, Z) p E (E_0 - E)^2 dE, \quad (10)$$

where  $p(E) = \sqrt{E^2 - 1}$  is the momentum of the  $\beta$  particle in units of  $m_e c^2$ ;  $E_0 = 1 + Q_{\beta^\pm}/m_e c^2$  is the total limit energy of  $\beta$  decay in units of  $m_e c^2$  (including the

electron rest mass);  $Q_{\beta^\pm}$  is the limit kinetic energy of  $\beta$  spectra;  $E = 1 + \varepsilon/m_e c^2$ ; and  $\varepsilon$  is the kinetic energy of the  $\beta$  particle.

The function  $F(E, Z)$  is determined by the magnitude of the radial electron (positron) wave function at the nuclear surface. Using the hydrogen-type relativistic wave functions Fermi has obtained the following relation, which is usually considered as the first approximation for the function  $F(E, Z)$

$$F_0(E, Z) = \frac{2(\gamma + 1)(2pR)^{2(\gamma-1)} \exp[\frac{\pi\xi}{p}] |\Gamma(\gamma + i\frac{\xi}{p})|^2}{\Gamma^2(2\gamma + 1)}, \quad (11)$$

where  $\alpha \simeq 1/137$  is the fine structure constant;  $\gamma = \sqrt{1 - \alpha^2 Z^2}$ ;  $\xi = \pm \alpha Z E$  (the upper sign corresponds to  $\beta^-$ -decay and the lower to  $\beta^+$ -decay);  $R$  is the nuclear radius in units of  $\hbar/m_e c$ ; and  $\Gamma$  is the gamma-function.

The screening effect from the orbital electrons has a large influence on the  $\beta$  electron (positron) wave function at the nuclear surface (especially for  $\beta^+$  decay). Usually it is taken into account by writing the function  $F$  as

$$F(E, Z) = F_0(E \mp V_0, Z) \mathfrak{a}^\mp(E \mp V_0, Z) \frac{p(E \mp V_0)(E \mp V_0)}{p(E)E}, \quad (12)$$

where  $V_0 = 1.81\alpha^2 Z^{4/3}$ ,<sup>57</sup> and  $\mathfrak{a}^\mp$  additionally takes into account the finite wavelength of the  $\beta$  particle, which is important for large  $Z$  and  $E$ .

### 2.3.2. Electron capture

The  $Q$ -value for EC process is determined as follows

$$Q_{EC} = M(A, Z) - M(A, Z - 1) - B_e = Q_{\beta^+} + 2m_e c^2 - B_e, \quad (13)$$

where  $B_e$  is the electron binding energy. Thus, it is possible that the EC can be energetically allowed even if the  $\beta^+$  decay is forbidden.

The main contribution to the EC process is given by the capture of K-electrons (nonrelativistic  $1s_{1/2}$  state). However, with increasing nuclear charge number, the contribution of the  $L$  orbit ( $L_I$  or nonrelativistic  $2s_{1/2}$  state and  $L_{II}$  or  $2p_{1/2}$  state) also increases and for  $Z \simeq 100$  this contribution is about 15–20%. The influence of higher orbits to the EC is negligible. Thus, the quantity  $f_0^{EC}$  is given by

$$f_0^{EC} = f_0^K + f_0^{L_I} + f_0^{L_{II}}, \quad (14)$$

where the Fermi function for the capture from a specific orbit  $X$  is

$$f_0^X = \frac{\pi}{2} [E(Q_{EC}) + E_X]^2 [g_X^2(Z_X) + f_X^2(Z_X)]. \quad (15)$$

Here  $E_X$  is the electron total energy

$$\begin{aligned} E_K &= \gamma, \\ E_L &= \left( \frac{1 + \gamma}{2} \right)^{1/2}. \end{aligned} \quad (16)$$

Using the effective charge  $Z_X$  takes approximately into account the screening of the nuclear Coulomb field by other electrons<sup>28</sup>

$$\begin{aligned} Z_K &= Z - 0.35, \\ Z_L &= Z - 4.15. \end{aligned} \quad (17)$$

Finally,  $g_X$  and  $f_X$  are the radial parts (taken at the nuclear surface) of the relativistic electron wave function of orbit  $X$ . Their nonzero components are

$$\begin{aligned} g_K^2(Z) &= \frac{4(1+\gamma)(2\alpha ZR)^{2\gamma-2}(\alpha Z)^3}{\Gamma(2\gamma+1)}, \\ g_{L_I}^2(Z) &= \frac{\left[(2\gamma+2)^{1/2}+2\right](2\gamma+1)(2\alpha ZR)^{2\gamma-2}(\alpha Z)^3}{\Gamma(2\gamma+1)\left[(2\gamma+2)^{1/2}+1\right](2\gamma+2)^\gamma}, \\ f_{L_{II}}^2(Z) &= \frac{3}{16}(\alpha Z)^2 g_{L_I}^2(Z). \end{aligned} \quad (18)$$

### 2.3.3. Comparison to experiment

We performed calculations of the half-lives with respect to the  $\beta$ -decay for the nuclei with known  $\beta$  half-lives. Figure 1 shows the ratio of the experimental half-lives to the calculated ones  $T_\beta^{\text{exp}}/T_\beta^{\text{th}}$  as a function of atomic number, experimental half-life

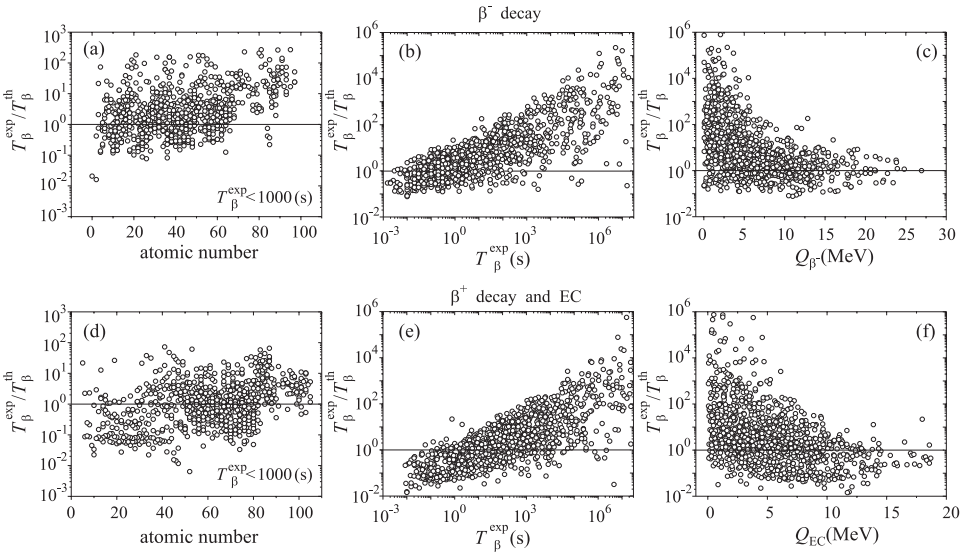


Fig. 1. Comparison of the experimental half-lives with the theoretical estimations for  $\beta^-$  (upper panels) and  $\beta^+ + \text{EC}$  (bottom panels) decays as a function of the atomic number of decaying nucleus [(a) and (d)], the experimental half-life [(b) and (e)], and the corresponding maximum energy release [(c) and (f)]. Only the nuclei having  $T_\beta^{\text{exp}} < 10^3$  s are shown on the panels (a) and (d) and having  $T_\beta^{\text{exp}} < 1$  year on the rest panels.

$T_{\beta}^{\text{exp}}$ , and the corresponding  $Q$ -value. The experimental data are from Refs. 58 and 59, only the nuclei with  $T_{\beta}^{\text{exp}} < 1 \text{ year} \simeq 3 \times 10^7 \text{ s}$  were considered. The increasing deviation as a function of  $T_{\beta}^{\text{exp}}$  indicates that large half-lives correspond to forbidden transitions, which we did not take into account. Better agreement of  $T_{\beta}^{\text{th}}$  with  $T_{\beta}^{\text{exp}}$  with increasing  $Q$ -values can be understood as follows. With increasing energy release, there is an increase of the probability to find an appropriate state (within the accessible energy range) fulfilling the conditions of allowed decay. On the other hand, for small  $Q$ -values there are very few states in the daughter nucleus accessible for the  $\beta$ -transitions, that could have spins and parities different from those of the parent nucleus, which results in forbidden  $\beta$ -decay. It is known that the dependence of the  $\beta$ -decay time on the energy release is much weaker than on the quantum numbers of initial and final states. Therefore, the ratio  $T_{\beta}^{\text{exp}}/T_{\beta}^{\text{th}}$  must tend to unity with increasing  $Q$ -value. This condition can be fulfilled if one takes the constant value of  $\log_{10} [f_0^b T_b]$  in Eq. (7) to be 4.7.

The  $\beta$ -decay half-lives shorter than 1000 s should be addressed to the allowed decays. Our calculations agree with the experiment within two orders of magnitude for  $T_{\beta}^{\text{exp}} < 1000 \text{ s}$ . This is sufficient to estimate the  $\beta$ -decay half-lives in competition with  $\alpha$ -decay and spontaneous fission almost for every experimentally unknown nucleus.

#### 2.4. Spontaneous fission

The spontaneous fission (SF) of nuclei is a very complicated process. Knowing the multidimensional potential energy surface only is not sufficient for the accurate determination of the corresponding decay time. The most realistic calculations of the SF half-life are based on the search for the least action path in the multidimensional deformation space. In addition a detailed knowledge of the collective inertia parameters is required. This constitutes an independent and complicated problem. Only few examples of such calculations are known.<sup>10,34–37</sup> Moreover, the analysis can be performed only in a rather restricted area of the nuclear map due to long calculation times. Thus, a preliminary estimation of the region on nuclear map, where SF plays an important role is necessary. One of the first systematics of the SF half-life based on the fission barrier heights and the values of the fissility parameter  $Z^2/A$  was proposed by Swiatecki.<sup>31</sup> After that many attempts were done to improve the SF half-life systematics (see, e.g. Refs. 32 and 33). Parameters of all such systematics were fitted to existing experimental data, which are very few, especially in the region of superheavy nuclei. Moreover, because of low statistics, experimental errors are often quite large in this region. It means that the predicting power of these systematics is under question for superheavy nuclei. In order to predict the general trend of the SF half-life and to fix the regions where SF plays a significant role we propose to employ the same idea as in Ref. 31 that the half-life is mainly determined by the barrier height on potential energy surface. However to determine the coefficients of the systematics we include in the fitting procedure



not only the experimental data<sup>63</sup> but also the realistic theoretical predictions<sup>34–36</sup> for the region  $100 \leq Z \leq 120$  and  $140 \leq N \leq 190$ . Thus, we propose to use the following relation for the SF half-life:

$$\begin{aligned} \log_{10} T_{SF} (\text{sec}) = & 1146.44 - 75.3153Z^2/A \\ & + 1.63792 (Z^2/A)^2 - 0.0119827 (Z^2/A)^3 \\ & + B_f (7.23613 - 0.0947022Z^2/A) \\ & + \begin{cases} 0, & Z \text{ and } N \text{ are even} \\ 1.53897, & A \text{ is odd} \\ 0.80822, & Z \text{ and } N \text{ are odd.} \end{cases} \end{aligned} \quad (19)$$

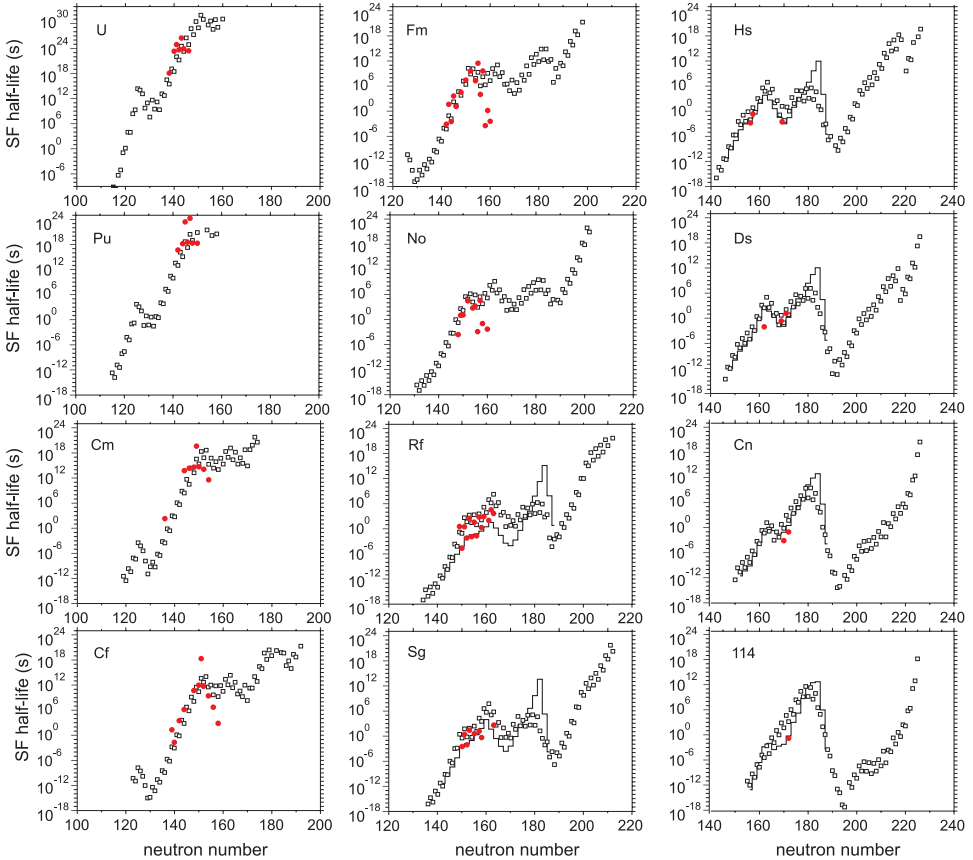


Fig. 2. (Color online). Dependence of the SF half-lives on the neutron number for the isotopes of elements from U to 114. The open black squares are the estimation by the phenomenological formula (19), the full red circles are the experimental data,<sup>59,63</sup> and the full lines are the calculations of Refs. 34 and 35.

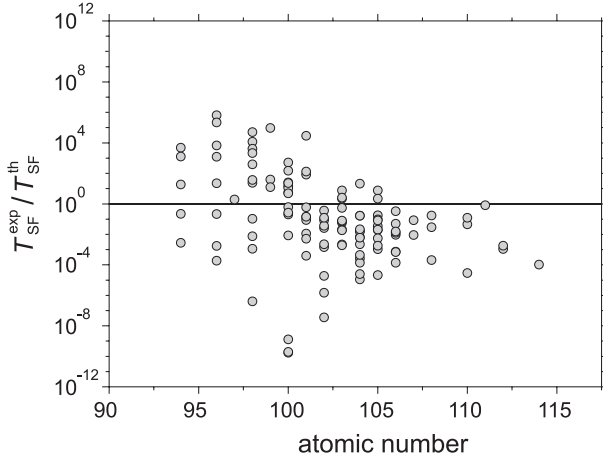


Fig. 3. The ratio of the experimental<sup>59,63</sup> SF half-lives to the calculated ones.

Here  $B_f$  is the fission barrier, which according to the topographical theorem<sup>60,61</sup> is calculated as a sum of the liquid-drop barrier  $B_f(LDM)$ <sup>62</sup> and the ground state shell correction  $\delta U(g.s.)$ , i.e.  $B_f = B_f(LDM) + \delta U(g.s.)$ . Figure 2 shows the dependence of the SF half-life on the neutron numbers for nuclei with even atomic numbers from uranium to  $Z = 114$  element. Obviously Eq. (19) qualitatively reproduces the behavior of the half-lives in the experimentally known region. However the proposed relation substantially underestimates the abrupt decrease of the half-life for californium, fermium, and nobelium around  $N = 160$ . In the region of superheavy nuclei we get reasonable agreement with the data. The quantitative agreement is seen in Fig. 3. Except for a few cases corresponding to the above mentioned neutron-rich isotopes of Cf, Fm, and No, the values of  $T_{SF}^{\text{exp}}/T_{SF}^{\text{th}}$  lie within six orders of magnitude. This result is quite understandable, because, as can be seen from Eq. (19), a disagreement of the barrier by 0.3 MeV leads to one order of magnitude deviation for the SF half-life. The accuracy of the macro-microscopical model in calculation of the fission barriers is  $\sim 1 - 2$  MeV, which explains the obtained agreement. The reason for larger deviation from the experimental SF half-lives for neutron-rich isotopes of Cf, Fm, and No is the influence of exit channel, caused by clusterization with two nearly double-magic tin fragments, which is a special case of this region of nuclei. This effect is not included in the relation (19), but is accounted for within the dynamical approach mentioned above. However, even in such advanced calculations, this steep decrease of the SF half-life is underestimated (see Fig. 4 in Ref. 36). In Fig. 2 we also show the calculations of Refs. 34, 35 for the isotopes of  $Z = 104 - 114$ . It is seen that in this region both models give similar results for those nuclei, for which experimental data exist. However, the model of Ref. 34, 35 predicts for some nuclei a too steep decrease of the half-lives around  $N \simeq 170$  and much longer times around the closed shell numbers  $N = 184$ .

One of the most important questions regarding the stability of the heaviest elements and the possibility of their synthesis in nature as well as in laboratories is the behavior of the SF half-lives for neutron-rich nuclei. The existing models predict an overall increase of the SF half-lives as a function of the neutron number. This is a pure macroscopic effect. The microscopical shell corrections lead to increasing half-lives while approaching the closed-shell numbers and decreasing in between. The amplitudes of this variation, of course, are very dependent on the model involved. The only way to check the accuracy of a model is to compare its predictions with the experiment. Unfortunately, there are not many experimental data for  $T_{SF}$  in the neutron-rich region. In particular it is important to have more experimental points on the neutron-rich side for the fermium region  $^{262-264}\text{Fm}$ , which builds a kind of bridge between rather stable actinides and the peninsula of stability at  $Z \simeq 108$ .

### 3. Stability of Heavy Nuclei

Figure 4 shows upper part of the nuclear maps of the total half-lives and decay modes for the nuclei with  $Z \leq 132$ . The known nuclei are situated along the  $\beta$ -stability line with a shift to the proton-rich region especially for heavy and superheavy nuclei. Almost all proton-rich nuclei with  $Z \leq 118$  having half-lives sufficiently long for their experimental identification are already synthesized. The red circles in Fig. 4 correspond to the nuclei with  $Z = 119-124$ , which may be obtained in the  $3n$  channel of the fusion reactions:  $^{50}\text{Ti} + ^{249}\text{Bk}$ ,  $^{50}\text{Ti} + ^{249}\text{Cf}$ ,  $^{54}\text{Cr} + ^{248}\text{Cm}$ ,  $^{54}\text{Cr} + ^{249}\text{Bk}$ ,  $^{54}\text{Cr} + ^{249}\text{Cf}$ ,  $^{58}\text{Fe} + ^{248}\text{Cm}$ ,  $^{58}\text{Fe} + ^{249}\text{Bk}$ , and  $^{58}\text{Fe} + ^{249}\text{Cf}$ . The synthesis cross-section of these new superheavy nuclei with  $Z > 118$  in fusion reactions is predicted to decrease substantially due to the change of the projectile from  $^{48}\text{Ca}$  to a heavier one.<sup>7</sup> Moreover, as can be seen from Figs. 4 and 5 these nuclei are very short-living. They are located at the border of  $1 \mu\text{s}$  area — the critical time required to pass separator to be detected. It means that the nuclei heavier than the 120 element — even if they will be synthesized — could be hardly detected because of their very short half-lives. This conclusion is model dependent. As was stated above, our calculations are based on the ground state masses. Figure 5 shows how the  $1 \mu\text{s}$  contour depends on the model used for the calculation. The contour line in Fig. 5(a) is obtained with the nuclear masses calculated by Möller *et al.*,<sup>44</sup> while Fig. 5(b) was calculated within the two-center shell model.<sup>51,52</sup> Both models give quite similar predictions of the half-lives for the nuclei which could be synthesized in the above written projectile-target combinations. However the borders of  $1 \mu\text{s}$  area on the neutron-rich side differ substantially for these two models. This discrepancy appears due to the extrapolation of the model parameters to the unknown region, while the results for experimentally studied nuclei are quite similar. The largest deviation appears for the predicted values of the fission barriers of superheavy nuclei. For example, the macro-microscopical approach<sup>64</sup> predicts the barrier  $B_f = 6.07 \text{ MeV}$  for  $^{302}120$  nucleus, while the microscopic models<sup>40</sup> give the

fission barrier for this nucleus in the range of 6–12 MeV depending on the nucleon–nucleon forces. Such a large fission barrier height will substantially increase the stability of the nucleus against SF. Unfortunately, the microscopic calculations<sup>40</sup> were performed only for few even–even superheavy nuclei. This fact does not allow us performing the systematic comparison of the predicted decay properties within the microscopic and macro-microscopic models. However, this uncertainty in the fission barriers (and correspondingly in the SF half-lives) does not alter our conclusion about perspectives of employing the fusion reactions for synthesis of new superheavy nuclei with  $Z = 119$ – $124$ , because the main decay mode of these nuclei is  $\alpha$ -decay (see Fig. 4).

The discovery of new elements mentioned above (even proton-rich isotopes) is certainly of interest. However, in our opinion, the most challenging region for future

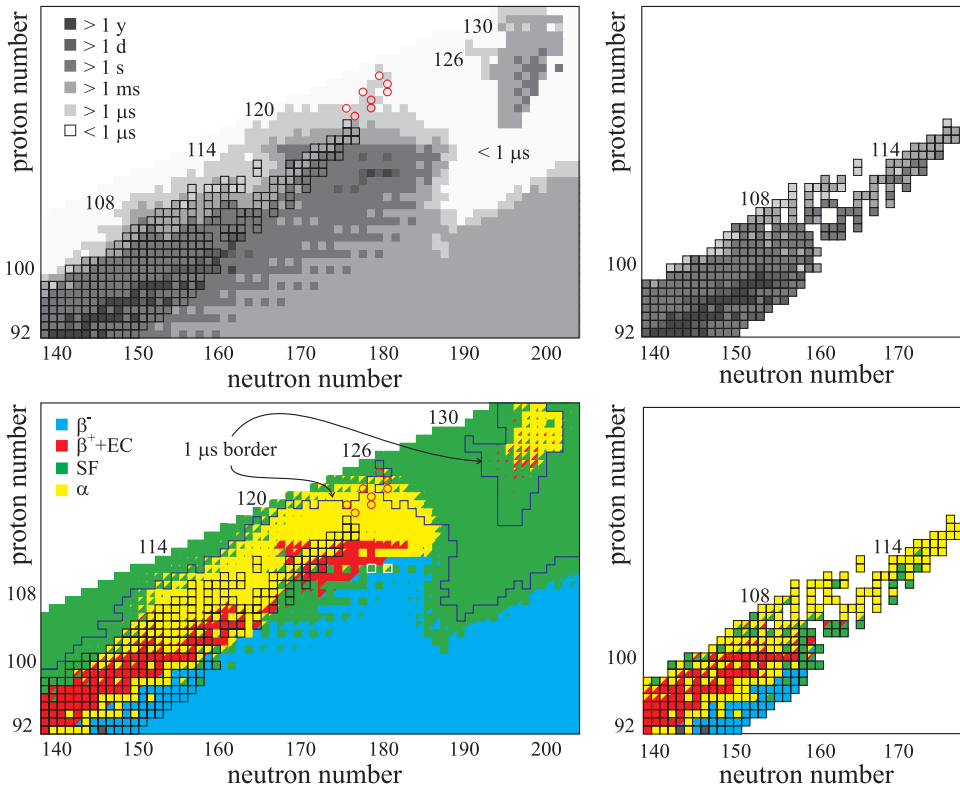


Fig. 4. (Color online). Maps of nuclei reflecting the total half-lives (top) and the decay modes (bottom). The left panels are calculations and the right panels are the experimental data taken from Refs. 58, 59. The contour lines on the left bottom panel correspond to the border of  $1 \mu\text{s}$  half-life. The circles show the nuclei with  $Z = 119$ – $124$ , which may be synthesized in the  $3n$  channel of fusion reactions  $^{50}\text{Ti} + ^{249}\text{Bk}$ ,  $^{249}\text{Cf}$  and  $^{54}\text{Cr}$ ,  $^{58}\text{Fe} + ^{248}\text{Cm}$ ,  $^{249}\text{Bk}$ ,  $^{249}\text{Cf}$  (see the text). The bounded cells correspond to the experimentally known nuclei. The bounded nuclei with the white color border are the most stable Copernicium isotopes  $^{291}\text{Cn}$  and  $^{293}\text{Cn}$ .

studies is the region of more heavy and more neutron-rich nuclei. This is especially the island of stability of superheavy nuclei centered at  $Z \sim 114$  and  $N \sim 184$  (remember, however, that the microscopic meson field theory also predicts nuclei around  $Z \sim 120$  and  $N \sim 184$  as a candidates for a stability island). According to our predictions the most long-living nuclei in the  $Z \sim 114$  and  $N \sim 184$  area are the  $\beta$ -stable isotopes of Copernicium  $^{291}\text{Cn}$  and  $^{293}\text{Cn}$  with the half-lives of about 100 years shown in Fig. 4 by the white-border squares. The main decay mode of  $^{291}\text{Cn}$  is predicted to be SF and  $^{293}\text{Cn}$  is decaying by  $\alpha$ -decay and SF with nearly equal probability. Because of their relatively long half-lives these isotopes — if synthesized — could be accumulated. Unfortunately these two isotopes are unreachable directly by any fusion reaction with stable ion beams. In principle, there is a chance to produce these nuclei in multi-nucleon transfer reactions.<sup>17</sup> However the corresponding cross-sections are very low. A new way for the synthesis of neutron-enriched superheavy nuclei and, in particular, those from the center of the stability island may be found basing on the found area of  $\beta^+$ -decaying nuclei in the vicinity of the island of stability (see below).

The possibility of existence of elements heavier than Uranium in nature remains still a highly discussed problem in nuclear physics. The probability of synthesis of superheavy nuclides during  $r$ -process depends very much on the decay properties of neutron-rich nuclei heavier than  $^{238}\text{U}$  as well as on the conditions (temperature, neutron flux, etc.) during supernova explosion, where the  $r$ -process is going on. Here we will not discuss such synthesis probabilities (see, e.g. Ref. 65 and references therein). Nevertheless, we mention that such superheavy nuclei being formed in  $r$ -processes could be found in nature if the decay time is long enough. Attempts to find the superheavy elements in terrestrial environment or in cosmic rays (see Refs. 4, 67 and 68 and references therein) were up to be now unsuccessful. Only an upper limit of the half-life  $5 \times 10^4$  years was determined by trying to observe the decay of Hs isotopes in Os samples, which is the chemical homologue of Hs.<sup>4</sup>

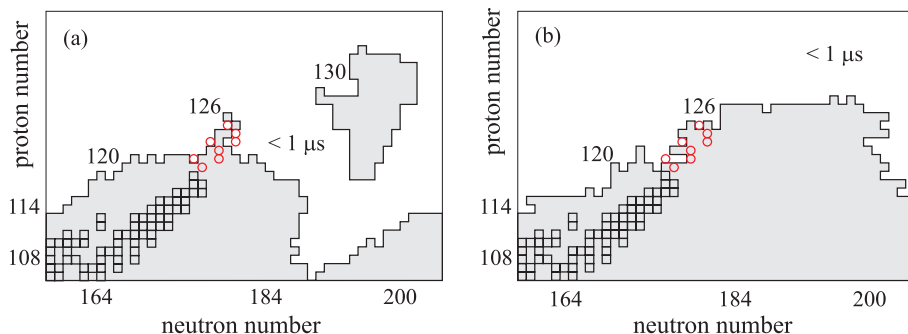


Fig. 5. The contour of  $1 \mu\text{s}$  half-life of superheavy nuclei obtained with ground state masses from Ref. 44 (a) and the two-center shell model (b). The squares show the known nuclei and the circles correspond to the nuclei with  $Z = 119$ – $124$  which may be synthesized in the  $3n$  channel of the fusion reactions  $^{50}\text{Ti} + ^{249}\text{Bk}$ ,  $^{249}\text{Cf}$  and  $^{54}\text{Cr}$ ,  $^{58}\text{Fe} + ^{248}\text{Cm}$ ,  $^{249}\text{Bk}$ ,  $^{249}\text{Cf}$  (see the text).

The longest half-life against  $\alpha$ -decay and SF is expected for  $^{292}\text{Hs}$  having the magic number of neutrons  $N = 184$ .<sup>34,35</sup> However, this isotope is  $\beta^-$ -unstable. According to our estimation the half-life of allowed  $\beta^-$ -decay of this isotope is about 7 s. The corresponding  $Q$ -value of 1.91 MeV is rather large to expect a strong suppression of  $\beta$ -transition with respect to allowed  $\beta$ -decays assumed here. Only two nuclei around  $Z = 40$  ( $^{98}\text{Tc}$  and  $^{94}\text{Nb}$ ) with close  $Q$ -values have  $T_{\beta^-}$  more than 100 years. Therefore, Hs isotopes most likely cannot be found in nature due to the short  $\beta^-$ -decay time. According to our predictions the experimental search for superheavy elements in nature could be focused on  $\beta$ -stable isotopes of Copernicium  $^{291}\text{Cn}$  and  $^{293}\text{Cn}$  having the longest half-lives. However these half-lives are about 100 years, which means that there are no chances to observe the decay of Cn in terrestrial environments. Instead the search could be made in cosmic rays.

It is now discussed that some of the Dubnium isotopes (i.e.  $^{268}\text{Db}$ ) are expected to be  $\beta^+$ -decaying, while only the SF mode was yet observed.<sup>4</sup> The corresponding experiments are planned to be performed to verify (or not) this prediction. We found that some isotopes of superheavy elements with  $111 \leq Z \leq 115$ , more neutron-rich than those synthesized recently in Dubna in the  $^{48}\text{Ca}$ -induced fusion reactions, also may undergo  $\beta^+$ -decay. Note, that the area of the  $\beta^+$ -decaying nuclei in the same region of the nuclear map was also obtained (but not discussed) in calculations of half-lives and decay modes by Koura *et al.*<sup>69–71</sup> The appearance of such an area of  $\beta^+$ -decaying nuclei in the vicinity of the island of stability becomes quite evident from the schematic Fig. 6. In this figure we consider the situation where

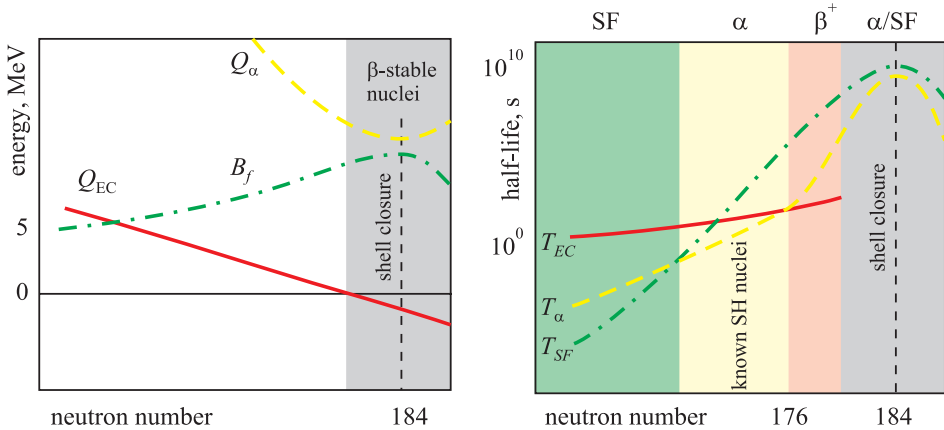


Fig. 6. Schematic picture explaining the existence of the region of  $\beta^+$ -decaying nuclei in the vicinity of the stability island. (left panel) Dependence on the neutron number of the characteristic energies of  $\beta^+$ -decay ( $Q_{EC}$ , solid curve), alpha-decay ( $Q_\alpha$ , dashed curve), and spontaneous fission ( $B_f$ , dash-dotted curve). The region of  $\beta$ -stable nuclei and the position of the neutron shell closure ( $N = 184$ ) are shown. (right panel) Expected behavior of the half-lives  $T_{EC}$  (solid curve),  $T_\alpha$  (dashed curve), and  $T_{SF}$  (dash-dotted curve) from the proton-rich side up to the center of the stability island. The dominating modes of decay and the position of known SH nuclei (in the vicinity of  $Z = 114$ ) are shown.

the neutron closure  $N = 184$  coincides with the region of  $\beta$ -stable nuclei (which is expected from the calculations of the nuclear masses close by the proton number  $Z = 114$ ). The left panel of Fig. 6 shows the typical behavior of the characteristic energies of EC,  $\alpha$ -decay, and SF playing the role in this region ( $Q_{\beta^-}$  is negative here and not shown). In this case one may expect the following order of decay modes starting from the proton drip line up to the top of the stability island (see the right panel in Fig. 6). Due to the strong Coulomb field, the most proton-rich nuclei should undergo SF with rather short half-lives. Moving to the “right” the fission barriers increase because of increase of the neutron number (and, therefore, decrease of the Coulomb forces) as well of the stabilizing effect of the neutron shell  $N = 184$ . Then  $\alpha$ -decay starts to play a main role. Note, that most nuclei known at the moment close to  $Z = 114$  (both synthesized in “cold” and “hot” fusion reactions) experience  $\alpha$ -decay. Approaching the island of stability the half-lives of  $\alpha$ -decay as well as those of SF increase by many orders of magnitude due to influence of the neutron shell  $N = 184$ . When these half-lives are longer than minutes and days (the typical half-lives with respect to EC of nuclei in the vicinity of the  $\beta$ -stability region), the EC process may dominate. Finally, the most stable nuclei (which should be  $\beta$ -stable) undergo  $\alpha$ -decay or/and SF. This consideration of the decay modes sequence is rather natural and model independent. It explains the area of  $\beta^+$ -decay found here. However, the size of this area depends on the nuclear masses and nuclear structure. It should be stressed ones more, that our calculations of  $\beta$ -decay half-lives are based on the assumption of allowed  $\beta$ -transitions. As was said above,  $\beta$ -decay can be substantially suppressed, especially for nuclei close to the  $\beta$ -stability line (i.e. having small  $Q$ -values of  $\beta$ -decays). This means that some of the nuclei found here to have the  $\beta^+$ -decay as the main mode, may have much longer  $\beta$ -decay time, whereas the main decay mode could be  $\alpha$ -decay or SF. However, the gross decay-mode structure of the nuclear map (i.e. existence of the region of  $\beta^+$ -decaying superheavy nuclei) remains. To perform more reliable calculations of  $T_\beta$  for a specific nucleus the structure of the mother and daughter nuclei are required. Presently, the information about the excited states of nuclei in the superheavy mass region is almost absent both theoretically and experimentally. Studies in this field will be demanding and interesting.

Our finding indicates that the experimental identification of the nuclei to the “right” of already discovered ones may meet significant difficulties. However, the existence of the area of  $\beta^+$ -decay gives us the hypothetic way (see Fig. 7) to produce  $^{291}\text{Cn}$  in the triple  $\beta^+$  (or EC) decay of  $^{291}115$  which in turn could be obtained, for example, after  $\alpha$ -decay of  $^{295}117$  in the reaction  $^{48}\text{Ca} + ^{249}\text{Bk} \rightarrow ^{295}117 + 2n$ . Recently<sup>5</sup> the element 117 has been discovered in the  $3n$  and  $4n$  evaporation channels of the fusion reaction  $^{48}\text{Ca} + ^{249}\text{Bk}$  with the cross-section  $\sim 1$  pb. Totally 6 events were registered. The predicted cross-section in the  $2n$  channel is  $\sim 0.3$  pb.<sup>7</sup> This means that at present only rare events could be registered in the  $2n$  channel, and the proposed method of reaching the island of stability hopefully may be

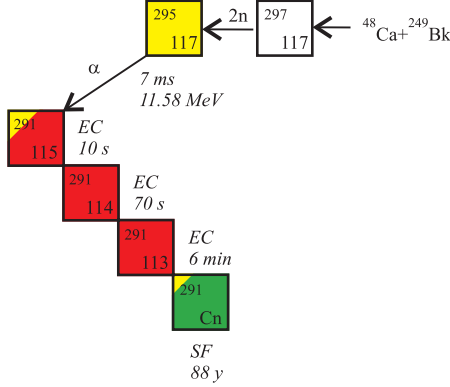


Fig. 7. The reaction and decay chain leading to the most stable nucleus on the island of stability  $^{291}\text{Cn}$ .

realized in future with the progress in experimental techniques. However, for the moment, this is the highest in cross-section method for production of the nuclei located in the middle of the first island of stability.

Another interesting region of nuclei (see Fig. 4) is situated in between  $120 \leq Z \leq 127$  and  $197 \leq N \leq 200$ . This region contains rather stable superheavy nuclei. It is well-separated from the known island of stability around  $Z = 114$ ,  $N = 184$  by the “gulf” of instability caused by SF and  $\alpha$ -decay, where the half-lives do not exceed  $1 \mu\text{s}$ . The nuclei within the new predicted area of relatively stable nuclei have half-lives of about 1 s. Their main decay modes are  $\alpha$ -decay and SF. However this prediction is model-dependent (mainly on the underlying shell model). For example, such an area does not appear within the two-center shell model (see Fig. 5). The main reason for existence of the found area of stability is the increase in the SF half-lives. This result is based on a rather simple phenomenological model for the SF process. In order to verify this finding more fundamental calculations should be made taking into account the dynamical effects and the multidimensional nature of the fission process. The possibility of experimental study of this region of the nuclear map is rather unclear. At least these nuclei are not accessible by fusion reactions.

#### 4. Conclusions

The study of half-lives of nuclei in a wide range of proton and neutron numbers is of great importance for understanding of nuclear properties as well as for the planning and analysis of experiments aimed to synthesis of new superheavy nuclei. We have calculated the nuclear decay properties (the decay modes and half-lives) for nuclei with  $Z \leq 132$ . The calculations are based on the phenomenological relations for the decay times and the ground-state masses and the shell corrections according to the macro-microscopic model<sup>44</sup> and those calculated within the two-center shell model.



The main decay modes have been taken into account, namely  $\alpha$ -decay,  $\beta^-$ -decay,  $\beta^+$ -decay, electron capture, and SF. For SF we proposed the phenomenological formula with the parameters defined from the fit to experimental data and the results of previous realistic calculations in the superheavy mass region.<sup>34–36</sup> The analysis of the obtained nuclear chart reveals a few important conclusions:

- (i) In accordance with our calculations the first island of stability of superheavy nuclei is centered at  $\beta$ -stable Copernicium isotopes  $^{291}\text{Cn}$  and  $^{293}\text{Cn}$  having the half-life of about 100 years.
- (ii) Because of such short half-lives the search in nature of these superheavy nuclei may be performed only in cosmic rays. Under terrestrial conditions a measurable amount of superheavies is unlikely to exist.
- (iii) At existing experimental facilities the synthesis and detection of nuclei with  $Z > 120$  produced in fusion reactions may be difficult (or impossible) due to their short half-lives (shorter than  $1 \mu\text{s}$ ). This prediction should be taken into account while planning new experiments and experimental setups.
- (iv) For the first time we found the area of  $\beta^+$ -decaying nuclei with  $111 \leq Z \leq 115$  located to the right of those synthesized in  $^{48}\text{Ca}$  fusion reactions. Hopefully in this region  $\alpha$ -decay dominates for the nuclei already discovered in the  $^{48}\text{Ca}$ -induced fusion reactions. The experimental identification of the more neutron-rich  $\beta^+$ -decaying isotopes of elements with  $111 \leq Z \leq 115$  is even more difficult. However, an existence of these nuclei gives us a chance to reach the center of the first island of stability in fusion reactions via  $\beta^+$ -decay chains similar to the one shown in Fig. 7.
- (v) We found the second region of rather stable superheavy nuclei at  $Z \sim 124$ ,  $N \sim 198$  with the maximum half-lives  $\sim 1$  s. It is separated from the “continent” by the “gulf” formed by nuclei with half-lives shorter than  $1 \mu\text{s}$ . However, the existence of this region is model dependent. For example, the shell model resulting from meson field theory<sup>16</sup> seems to be quite different from the simple extrapolation of the naive Mayer–Jensen shell model. A more detailed analysis of decay properties of nuclei in this area is required especially for the SF process. One should also remember that the extrapolation of the underlying shell model into the new domain of nuclei is not clear yet.

## Acknowledgment

This work was supported in part by DFG-RFBR collaboration and Helmholtz association. One of us (A.V.K.) is indebted to JINR for support of these studies within the young scientist grant program. Two of us (Y.M.P. and L.F.R.) are grateful to the DAAD for a PhD stipend.

## References

1. S. Hofmann and G. Münzenberg, *Rev. Mod. Phys.* **72** (2000) 733.

2. K. Morita, K. Morimoto, D. Kaji, T. Akiyama, S. Goto, H. Haba, E. Ideguchi, K. Katori, H. Koura, H. Kudo, T. Ohnishi, A. Ozawa, T. Suda, K. Sueki, F. Tokanai, T. Yamaguchi, A. Yoneda and A. Yoshida, *J. Phys. Soc. Jpn.* **76** (2007) 043201.
3. K. Morita, K. Morimoto, D. Kaji, T. Akiyama, S. Goto, H. Haba, E. Ideguchi, K. Katori, H. Koura, H. Kikunaga, H. Kudo, T. Ohnishi, A. Ozawa, N. Sato, T. Suda, K. Sueki, F. Tokanai, T. Yamaguchi, A. Yoneda and A. Yoshida, *J. Phys. Soc. Jpn.* **76** (2007) 045001.
4. Y. Oganessian, *J. Phys. G* **34** (2007) R165.
5. Yu. Ts. Oganessian, F. Sh. Abdullin, P. D. Bailey, D. E. Benker, M. E. Bennett, S. N. Dmitriev, J. G. Ezold, J. H. Hamilton, R. A. Henderson, M. G. Itkis, Yu. V. Lobanov, A. N. Mezentsev, K. J. Moody, S. L. Nelson, A. N. Polyakov, C. E. Porter, A. V. Ramayya, F. D. Riley, J. B. Roberto, M. A. Ryabiniin, K. P. Rykaczewski, R. N. Sagaidak, D. A. Shaughnessy, I. V. Shirokovsky, M. A. Stoyer, V. G. Subbotin, R. Sudowe, A. M. Sukhov, Yu. S. Tsyganov, V. K. Utyonkov, A. A. Voinov, G. K. Vostokin and P. A. Wilk, *Phys. Rev. Lett.* **104** (2010) 142502.
6. Yu. Ts. Oganessian, V. K. Utyonkov, Yu. V. Lobanov, F. Sh. Abdullin, A. N. Polyakov, R. N. Sagaidak, I. V. Shirokovsky, Yu. S. Tsyganov, A. A. Voinov, G. G. Gulbekian, S. L. Bogomolov, B. N. Gikal, A. N. Mezentsev, S. Iliev, V. G. Subbotin, A. M. Sukhov, K. Subotic, V. I. Zagrebaev, G. K. Vostokin, M. G. Itkis, K. J. Moody, J. B. Patin, D. A. Shaughnessy, M. A. Stoyer, N. J. Stoyer, P. A. Wilk, J. M. Kenneally, J. H. Landrum, J. F. Wild and R. W. Lougheed, *Phys. Rev. C* **74** (2006) 044602.
7. V. I. Zagrebaev and W. Greiner, *Phys. Rev. C* **78** (2008) 034610.
8. U. Mosel, B. Fink and W. Greiner, in *Memorandum zur Errichtung eines gemeinsamen Ausbildungszentrums für Kernphysik der Hessischen Hochschulen* (Darmstadt, Frankfurt am Main, and Marburg, 1966).
9. H. Meldner, Ph.D. thesis, University Frankfurt am Main (1966); see also *Proc. Int. Symp. Why and How Should We Investigate Nuclides Far Off the Stability Line*, Lysekil, Sweden, 1966.
10. U. Mosel and W. Greiner, *Z. Phys.* **222** (1969) 261.
11. S. G. Nilsson, C. F. Tsang, A. Sobiczewski, Z. Szymanski, S. Wycech, C. Gustafson, I.-L. Lamm, P. Möller and B. Nilsson, *Nucl. Phys. A* **131** (1969) 1.
12. Z. Patyk and A. Sobiczewski, *Nucl. Phys. A* **533** (1991) 132.
13. P. Möller and J. R. Nix, *Nucl. Phys. A* **549** (1992) 84.
14. M. Beiner, H. Flocard, M. Vénéroni and P. Quentin, *Phys. Scripta A* **10** (1974) 84.
15. S. Ćwiok, J. Dobaczewski, P. H. Heenen, P. Magierski and W. Nazarewicz, *Nucl. Phys. A* **611** (1996) 211.
16. K. Rutz, M. Bender, T. Bürvenich, T. Schilling, P. G. Reinhard, J. A. Maruhn and W. Greiner, *Phys. Rev. C* **56** (1997) 238.
17. V. I. Zagrebaev, Yu. Ts. Oganessian, M. G. Itkis and W. Greiner, *Phys. Rev. C* **73** (2006) 031602.
18. V. I. Zagrebaev and W. Greiner, *J. Phys. G* **35** (2008) 125103.
19. A. Sobiczewski, Z. Patyk and S. Ćwiok, *Phys. Lett. B* **224** (1989) 1.
20. A. Sobiczewski, *Russ. Chem. Rev.* **78** (2009) 1111.
21. Yu. Ts. Oganessian, V. K. Utyonkov, Yu. V. Lobanov, F. Sh. Abdullin, A. N. Polyakov, I. V. Shirokovsky, Yu. S. Tsyganov, G. G. Gulbekian, S. L. Bogomolov, B. N. Gikal, A. N. Mezentsev, S. Iliev, V. G. Subbotin, A. M. Sukhov, A. A. Voinov, G. V. Buklanov, K. Subotic, V. I. Zagrebaev, M. G. Itkis, J. B. Patin, K. J. Moody, J. F. Wild, M. A. Stoyer, N. J. Stoyer, D. A. Shaughnessy, J. M. Kenneally, P. A. Wilk, R. W. Lougheed, R. I. Ilkaev and S. P. Vesnovskii, *Phys. Rev. C* **70** (2004) 064609.
22. D. N. Poenaru, I. H. Plonski and W. Greiner, *Phys. Rev. C* **74** (2006) 014312.

23. C. Samanta, P. R. Chowdhury and D. N. Basu, *Nucl. Phys. A* **789** (2007) 142.
24. M. Ismail, A. Y. Ellithi, M. M. Botros and A. Adel, *Phys. Rev. C* **81** (2010) 024602.
25. E. O. Fiset and J. R. Nix, *Nucl. Phys. A* **193** (1972) 647.
26. P. Möller, J. R. Nix and K.-L. Kratz, *Atom. Data Nucl. Data Tables* **66** (1997) 131.
27. B. W. Sargent, *Proc. R. Soc. London Ser. A* **139** (1933) 659.
28. M. A. Preston, *Physics of the Nucleus* (Addison-Wesley Publishing Company, Inc., Reading, Massachusetts, 1962), p. 574.
29. X. Zhang and Z. Ren, *Phys. Rev. C* **73** (2006) 014305.
30. X. Zhang, Z. Ren, Q. Zhi and Q. Zheng, *J. Phys. G* **34** (2007) 2611.
31. W. J. Swiatecki, *Phys. Rev.* **100** (1955) 937.
32. D. W. Dorn, *Phys. Rev.* **121** (1961) 1740.
33. C. Xu and Z. Ren, *Phys. Rev. C* **71** (2005) 014309.
34. R. Smolańczuk, *Phys. Rev. C* **56** (1997) 812.
35. R. Smolańczuk, J. Skalski and A. Sobiczewski, *Phys. Rev. C* **52** (1995) 1871.
36. A. Staszczak, Z. Lojewski, A. Baran, B. Nerlo-Pomorska and K. Pomorski, *Proc. Third Int. Conf. Dynamical Aspects of Nuclear Fission*, Casta-Papernicka, August 30–September 4, 1996, p. 22.
37. A. Sobiczewski and K. Pomorski, *Prog. Part. Nucl. Phys.* **58** (2007) 292.
38. P. Möller, J. R. Nix and W. J. Swiatecki, *Nucl. Phys. A* **469** (1987) 1.
39. A. Mamdouh., J. M. Pearson, M. Rayet and F. Tondeur, *Nucl. Phys. A* **644** (1998) 389; **648** (1999) 282(E); **679** (2001) 337.
40. T. Bürvenich, M. Bender, J. A. Maruhn and P.-G. Reinhard, *Phys. Rev. C* **69** (2004) 014307.
41. H. Goutte, J. F. Berger, P. Casoli and D. Gogny, *Phys. Rev. C* **71** (2005) 024316.
42. V. M. Strutinsky, *Nucl. Phys. A* **95** (1967) 420; **22** (1968) 1.
43. M. Brack, J. Damgaard, A. S. Jensen, H. C. Pauli, V. M. Strutinsky and C. Y. Wong, *Rev. Mod. Phys.* **44** (1972) 320.
44. P. Möller, J. R. Nix, W. D. Myers and W. J. Swiatecki, *Atom. Data Nucl. Data Tables* **59** (1995) 185.
45. V. V. Pashkevich, *Nucl. Phys. A* **169** (1971) 275.
46. S. Ćwiok, V. V. Pashkevich, J. Dudek and W. Nazarewicz, *Nucl. Phys. A* **410** (1983) 254.
47. S. Ćwiok, Z. Lojewski and V. V. Pashkevich, *Nucl. Phys. A* **444** (1985) 1.
48. V. V. Pashkevich, *Nucl. Phys. A* **477** (1988) 1.
49. A. Baran, K. Pomorski, A. Lukasiak and A. Sobiczewski, *Nucl. Phys. A* **361** (1981) 83.
50. Z. Patyk, J. Skalski, A. Sobiczewski and S. Ćwiok, *Nucl. Phys. A* **502** (1989) 591c.
51. J. Maruhn and W. Greiner, *Z. Phys. A* **251** (1972) 431.
52. V. I. Zagrebaev, A. V. Karpov, Y. Aritomo, M. Naumenko and W. Greiner, *Phys. Part. Nucl.* **38** (2007) 469.
53. V. E. Viola and G. T. Seaborg, *J. Inorg. Nucl. Chem.* **28** (1966) 741.
54. J. M. Eisenberg and W. Greiner, *Nuclear Theory*, Vol. 2 (North-Holland, 1988), p. 516.
55. B. S. Dzhelepov, L. N. Zyryanova and Yu. P. Suslov, *Beta Processes, Functions for the Analysis of Beta Spectra and Electron Capture* (Nauka, Leningrad, 1972), p. 373 [in Russian].
56. C. S. Wu and S. A. Moszkowski, *Beta Decay* (John Wiley & Sons, New York, 1966), p. 183.
57. R. P. Feynman, N. Metropolis and E. Teller, *Phys. Rev.* **75** (1949) 1561.
58. G. Audi, O. Bersillon, J. Blachot and A. H. Wapstra, *Nucl. Phys. A* **729** (2003) 3.

59. V. I. Zagrebaev, A. S. Denikin, A. V. Karpov, A. P. Alekseev, V. V. Samarin, M. A. Naumenko and V. A. Rachkov, *Nuclear Map of NRV*, <http://nrw.jinr.ru/nrv>.
60. W. D. Myers and W. J. Swiatecki, *Nucl. Phys. A* **601** (1996) 141.
61. A. V. Karpov, A. Kelić and K.-H. Schmidt, *J. Phys. G* **35** (2008) 035104.
62. A. J. Sierk, *Phys. Rev. C* **33** (1986) 2039.
63. N. E. Holden and D. C. Hoffman, *Pure Appl. Chem.* **72** (2000) 1525.
64. P. Möller, A. J. Sierk, T. Ichikawa, A. Iwamoto, R. Bengtsson, H. Uhrenholt and S. Åberg, *Phys. Rev. C* **79** (2009) 064304.
65. I. V. Panov, I. Yu. Korneev and F.-K. Thielemann, *Yad. Fiz.* **72** (2009) 1070.
66. I. V. Panov, I. Yu. Korneev and F.-K. Thielemann, *Phys. Atom. Nucl.* **72** (2009) 1026.
67. G. N. Flerov and G. M. Ter-Akopian, *Rep. Prog. Phys.* **46** (1983) 817.
68. G. N. Flerov and G. M. Ter-Akopian, in *Treatise on Heavy-Ion Physics*, Vol. 4, ed. D. A. Bromley (New York, Plenum, 1985), p. 333.
69. F. Dellinger, W. Kutschera, O. Forstner, R. Golser, A. Priller, P. Steier, A. Wallner and G. Winkler, *Phys. Rev. C* **83** (2011) 015801.
70. H. Koura, in *Proc. V Tours Symposium on Nuclear Physics*, eds. M. Arnould et al. (Tours, France, 2003) (AIP, 2004) p. 60.
71. H. Koura and T. Tachibana, *Nippon Butsuri Gakkai-shi*, **60** (2005) 717 (in Japanese) [[http://jolisfukyu.tokai-sc.jaea.go.jp/fukyu/mirai-en/2006/6\\_3.html](http://jolisfukyu.tokai-sc.jaea.go.jp/fukyu/mirai-en/2006/6_3.html)].